Structural Engineering and Mechanics, *Vol. 50, No. 1 (2014) 53-71*
DOI: http://dx.doi.org/10.12989/sem.2014.50.1.053

Dynamic behavior of a functionally graded plate resting on Winkler elastic foundation and in contact with fluid

Ali A. Shafiee[*1], Farhang Daneshmand[2a], Ehsan Askari[3b] and Mojtaba Mahzoon[1c]

[1]*Faculty of Mechanical Engineering, Shiraz University, Shiraz 71348-51154, Iran*
[2]*Department of Mechanical Engineering, McGill University, 817 Sherbrooke Street W., Montreal, Québec H3A 2K6, Canada*
[3]*Australian School of Advanced Medicine, Macquarie University, Sydney, Australia*

(Received April 5, 2013, Revised July 29, 2013, Accepted February 1, 2014)

Abstract. A semi-analytical method is developed to consider free vibrations of a functionally graded elastic plate resting on Winkler elastic foundation and in contact with a quiescent fluid. Material properties are assumed to be graded distribution along the thickness direction according to a power-law in terms of the volume fractions of the constituents. The fluid is considered to be incompressible and inviscid. In the analysis, the effect of an in-plane force in the plate due to the weight of the fluid is taken into account. By satisfying the compatibility conditions along the interface of fluid and plate, the fluid-structure interaction is taken into account and natural frequencies and mode shapes of the coupled system are acquired by employing energy methods. The results obtained from the present approach are verified by those from a finite element analysis. Besides, the effects of volume fractions of functionally graded materials, Winkler foundation stiffness and in-plane forces on the dynamic of plate are elucidated.

Keywords: dynamic behavior; fluid-structure interaction; functionally graded material; Winkler elastic foundation; in-plane forces

1. Introduction

Free vibration analysis of circular plates made of composite materials such as functionally graded materials (FGM) is of interest in practical applications. Functionally graded materials have appeal properties of high strength, minimum weight and ultra-high temperature resistance and were first introduced by a group of Japanese scientists (Shen 2009). A typical FGM, is an inhomogeneous composite made of different phases of material constituents usually metal and ceramic with a high bending-stretching coupling effect was reported by Shen (2009). By gradually varying the volume fraction of constituent materials, the material properties of functionally graded materials vary smoothly and change continuously between different layers. This advantage eliminates interface problems of composite materials and the stress distribution becomes smooth.

*Corresponding author, Ph.D. Student, E-mail: aa.shafiee@me.iut.ac.ir, aa.shafiee@yahoo.com
[a]Professor, E-mail: farhang.daneshmand@mcgill.ca
[b]Ph.D. Student, E-mail: ehsanaskary@gmail.com
[c]Professor, E-mail: mahzoon@shirazu.ac.ir

http://www.techno-press.org/?journal=sem&subpage=8 ISSN: 1225-4568 (Print), 1598-6217 (Online)

FGMs now have been regarded as one of the most promising candidates for future intelligent composites in many engineering fields such as spacecraft thermal shield structures, heat exchanger tubes, biomedical implants, flywheels, fusion reactors, blades, storage tanks, pressure vessels, and general wear and corrosion resistant coatings or for joining dissimilar materials in aerospace, automobile and defense industries.

Several researchers have focused their attention on investigating the dynamics of the FGM components under mechanical loads. Yang and Shen (2001) considered the dynamic response of initially stressed functionally graded rectangular thin plates subjected to impulsive lateral loads. Linear and nonlinear thermo-mechanical response of FGM plates subjected to static and dynamic loads has been studied with a third-order plate theory and a displacement finite element model was reported by Aliaga and Reddy (2004). The effects of amplitude of vibration, initial condition and volume fraction on nonlinear vibration of FGM plates with arbitrary initial stresses have been studied by Chun-Sheng (2005). Nie and Zhong (2007) investigated three-dimensional free and forced vibration analysis of functionally graded circular plate with various boundary conditions. They used three-dimensional theory of elasticity. A semi-analytical approach for nonlinear free and forced axisymmetric vibration of a thin circular functionally graded plate was developed by Allahverdizadeh *et al*. (2008). Nonlinear vibration of hybrid composite plates on elastic foundations have been studied by Chen *et al*. (2011). Rad (2012) investigated the static behavior of bi-directional functionally graded (FG) non-uniform thickness circular plate resting on quadratically gradient elastic foundations subjected to axisymmetric transverse and in-plane shear. Thermomechanical bending response of FGM thick plates resting on Winkler-Pasternak elastic foundations were considered by Bouderba *et al*. (2013).

Coupled vibration of a flexible circular plate made of functionally graded material is studied in the present paper. The plate is considered to be in contact with fluid and resting on a Winkler elastic foundation as a model of soil foundation. The effect of in-plane forces because of static fluid pressure is also considered. In order to formulate such a full coupled vibration problem, a semi-analytical approach based on energy methods is developed. Amabili and Dalpiaz (1998) studied the free vibrations of based plates in annular cylindrical tanks theoretically and experimentally. The combined effect of thickness variation and hydrostatic in-plane force on the natural frequencies of a circular plate has been studied by Jain (1972) on the basis of the classical plate theory. Jeong (2003) presented a theoretical method which was based on the finite Fourier-Bessel series expansion and the Rayleigh-Ritz method to investigate the fluid-coupled vibration of two identical circular plates. Ergin and U?urlu (2003) considered the hydroelastic vibration of a cantilever plate partially submerged in a fluid. Chan Il (1992) derived the frequency equation for the in-plane vibration of the clamped circular plate of uniform thickness with an isotropic material in the elastic range. Free vibrations of rectangular Mindlin plates resting on Pasternak foundation and in contact with fluid were considered by Hosseini-Hashemi *et al*. (2010). Askari and Daneshmand (2010) developed an analytical method to investigate the effect of internal bodies on the hydroelastic vibration of circular plates. Kutlu *et al*. (2012) considered the free vibration of moderately thick plates which rest on arbitrarily orthotropic two parameter foundation. They employed finite element method to analysis the Mindlin plate and Pasternak foundation and boundary element approach to model the fluid.

Material properties are assumed to be graded distribution along the thickness direction according to a power-law in terms of the volume fractions of the constituents. The clamped boundary condition is assumed for the circular plate. The fluid is assumed to be incompressible and inviscid and the velocity potential is formulated in terms of Bessel functions and sinusoidal

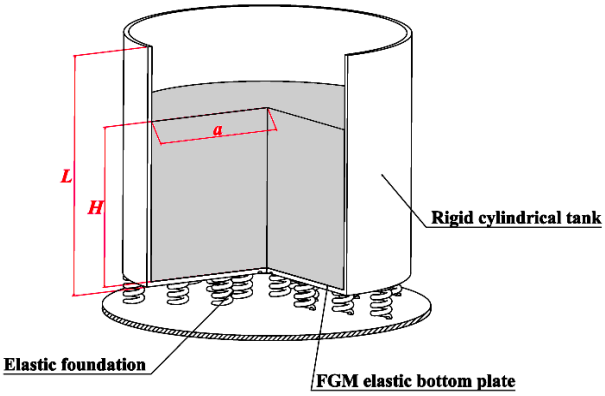

Fig. 1 A FGM elastic bottom plate in contact with fluid and resting on a Winkler elastic foundation

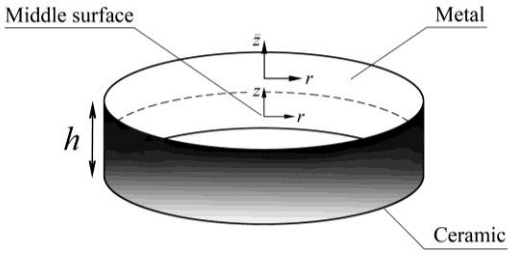

Fig. 2 Geometry and coordinate system of the FGM plate

functions. Applying compatibility conditions on the fluid and structure interface, the Rayleigh–Ritz method is utilized to calculate the natural frequencies and modes of the plate. The validity of the proposed method is verified by comparing the results with those obtained from the experimental and numerical solutions. A finite element analysis is also used to check the validity of the present method. The effects of volume fractions (material parameter) of functionally graded materials, Winkler foundation stiffness, fluid level, thickness of the plate, the number of nodal diameters and circles and the in-plane force on the natural frequencies of the coupled system are also examined.

2. The governing equations

Consider a functionally graded elastic bottom plate of a partially fluid-filled cylindrical tank resting on Winkler elastic foundation as shown in Fig. 1 The rigid tank has radius a, length L, elastic thin plate of thickness h and is filled to a height of H with an inviscid incompressible fluid of mass density ρ_L. The plate is assumed to be made of a functionally graded material. The radial, circumferential and axial coordinates are denoted by r, θ and z, respectively.

2.1 The material properties of the FGM plate

The functionally graded material (FGM) can be defined by the variation in the volume fractions, which is described by the power-law function.

For the elastic circular plate shown in Fig. 2, the z- and $\bar{z}$ -axis are on the middle surface and top surface of the plate, respectively. The Young's modulus and mass density of the plates vary continuously in the thickness direction (z-axis) i.e., $E=E(z)$, $\rho=\rho(z)$. The effect of Poisson's ratio on the deformation is much less than that of Young's modulus and a constant Poisson's ratio is assumed in the present study. However, the Young's modulus and mass density of the FGM plate vary in z-direction with power-law functions (P-FGM). The local volume fraction of the P-FGM is assumed to obey a power-law function

$$G(z)=\left(\frac{z+h/2}{h}\right)^{p} \tag{1}$$

where p is the material parameter and h is the thickness of the plate. The material properties of a P-FGM are determined by the rule of mixture (Ebrahimi *et al*. 2011)

$$\begin{aligned} E(z) &= G(z)E_m + [1-G(z)]E_c \\ \rho(z) &= G(z)\rho_m + [1-G(z)]\rho_c \end{aligned} \tag{2}$$

where E_m and ρ_m are the Young's modulus and mass density of the plate at the top surface, $z = h/2$ and $\bar{z}=0$. Similarly, E_c and ρ_c are the Young's modulus and mass density of the FGM plate at the bottom surface and $z = -h/2$, respectively.

2.2 Kinetic and potential energies for a plate

The Rayleigh-Ritz method is applied to find the natural frequencies and modes of the plate, and the time variation is assumed to be harmonic. Assuming the eigenfunctions of the clamped circular plate in vacuo as admissible functions, the transverse deflection W of the plate coupled to the fluid can be written as (Leissa 1969)

$$W(r,\theta)=\cos(n\theta)\sum_{i=0}^{\infty} q_i\left[J_n\left(\frac{\lambda_{ni}r}{a}\right)+A_{ni}I_n\left(\frac{\lambda_{ni}r}{a}\right)\right] \tag{3}$$

where n and i are the number of nodal diameters and circles, respectively, a is the plate radius, q_i are the parameters of the Ritz expansion, λ_{ni} is the well-known frequency parameter related to the plate natural frequency, J_n and I_n are the Bessel function and modified Bessel function of order n, respectively. λ_{ni} are frequency parameters and can be obtained as (Leissa 1969)

$$J_n(\lambda_{ni})I_n'(\lambda_{ni})-J_n'(\lambda_{ni})I_n(\lambda_{ni})=0 \tag{4}$$

where J'_n and I'_n indicate the r-derivatives of J_n and I_n. The mode shape constant for clamped plates is defined as

$$A_{ni}=-\frac{I_n(\lambda_{ni})}{J_n(\lambda_{ni})} \tag{5}$$

The reference kinetic energy T^*_P of the plate can be written as (Askari and Daneshmand 2010)

$$T_P^*=\frac{1}{2}\int_{-h/2}^{h/2}\int_0^{2\pi}\int_0^a \rho(z)W^2 r\,dr\,d\theta\,dz \tag{6}$$

Substituting Eqs. (2)-(3) and (5) in Eq. (6), the reference kinetic energy of FGM plate T^*_P becomes

$$T_P^* = \frac{1}{2}\left(\rho_c h + \frac{h(\rho_m - \rho_c)}{(p+1)}\right) a^2 \psi_n \sum_{i=0}^{\infty} q_i^2 \tag{7}$$

where

$$\psi_n = \begin{cases} 2\pi & if \quad n = 0 \\ \pi & if \quad n > 0 \end{cases} \tag{8}$$

The maximum potential energy of the plate is the summation of the reference kinetic energies of the eigenfunctions of the plate in vacuum multiplied by ω_{ni}^2 , i.e.

$$\begin{aligned} U_P = \frac{1}{2}\left(\rho_c h + \frac{h(\rho_m - \rho_c)}{(p+1)}\right) a^2 \psi_n \sum_{i=0}^{\infty} q_i^2 \omega_{ni}^2 = \\ \frac{1}{2a^2}\left(\frac{E_c h^3}{12(1-\nu^2)} + \frac{h^3(E_m - E_c)(p^2 - p + 2)}{4(1-\nu^2)(p+1)(p+2)(p+3)}\right) \psi_n \sum_{i=0}^{\infty} q_i^2 \lambda_{ni}^4 \end{aligned} \tag{9}$$

where the plate circular frequency ω_{ni} is related to the frequency parameter by λ_{ni}

$$\omega_{ni} = \frac{\lambda_{ni}^2}{a^2} \sqrt{\frac{\dfrac{E_c h^3}{12(1-\nu^2)} + \dfrac{h^3(E_m - E_c)(p^2 - p + 2)}{4(1-\nu^2)(p+1)(p+2)(p+3)}}{\rho_c h + \dfrac{h(\rho_m - \rho_c)}{(p+1)}}} \tag{10}$$

The maximum potential energy stored by the Winkler elastic foundation is also given by Amabili (1997).

$$U_E = \frac{1}{2} k' \int_0^{2\pi} \int_0^a W^2 r dr d\theta = \frac{1}{2} k' \psi_n a^2 \sum_{i=0}^{\infty} q_i^2 \tag{11}$$

where $k^{'}$ is the stiffness of the foundation.

The effect of in-plane load on the bottom plate due to the weight of the fluid is included in the study. The maximum potential energy associated with flexural vibrations of the plate as a consequence of in-plane load is (Gunaratnam and Bhattacharya 1985)

$$U_I = \frac{1}{2} \int_0^{2\pi} \int_0^a N_{ipl} \left\{ \left(\frac{\partial w_p}{\partial r}\right)^2 + \left(\frac{1}{r}\frac{\partial w_p}{\partial \theta}\right)^2 \right\} r dr d\theta \tag{12}$$

where for P-FGM plate

$$\begin{aligned} U_I = \frac{1}{2} \psi_n \sum_{i-0}^{\infty} \sum_{h=0}^{\infty} q_i q_h \left(\frac{\lambda_{ni}\lambda_{nh}}{a^2} \int_0^a N_{ipl} \left[A_{ni} J_n'\left(\lambda_{ni}\frac{r}{a}\right) + C_{ni} I_n'\left(\lambda_{ni}\frac{r}{a}\right)\right] \times \left[A_{nh} J_n'\left(\lambda_{nh}\frac{r}{a}\right) + C_{nh} I_n'\left(\lambda_{nh}\frac{r}{a}\right)\right] r dr + \\ n^2 \int_0^a N_{ipl} \left[A_{ni} J_n\left(\lambda_{ni}\frac{r}{a}\right) + C_{ni} I_n\left(\lambda_{ni}\frac{r}{a}\right)\right] \times \left[A_{nh} J_n\left(\lambda_{nh}\frac{r}{a}\right) + C_{nh} I_n\left(\lambda_{nh}\frac{r}{a}\right)\right] \frac{dr}{r}\right) \end{aligned} \tag{13}$$

where N_{ipl} is the in-plane load for unit length

$$N_{ipl}=\frac{f^2\int_{-h/2}^{h/2}E(z)dz}{6a^2}\left(3-6\left(\frac{r}{a}\right)^2+4\left(\frac{r}{a}\right)^4-\left(\frac{r}{a}\right)^6\right)$$
$$f=\frac{\rho g H a^2}{64\int_{-h/2}^{h/2}\frac{E(z)}{(1-\nu^2)}z^2dz} \tag{14}$$

2.3 Dynamic behavior of the fluid-structure interaction

The tank is partially filled with an inviscid and incompressible fluid whose the free surface is at distance H from the bottom plate (Fig. 1). For an incompressible and inviscid fluid the deformation potential satisfies the Laplace equation as follows

$$\nabla^2\varphi(r,\theta,\bar{z})=0 \tag{15}$$

The deformation potential φ is related to the velocity potential $\tilde{\varphi}$ by

$$\tilde{\varphi}(r,\theta,\bar{z},t)=-i\omega\varphi e^{i\omega t} \quad , \quad i^2=-1 \tag{16}$$

where ω is the natural circular frequency of vibration. Along the contact surface between the plate and fluid, the normal velocity of the fluid and the normal velocity of the plate must be equal. This is the condition of contact between the plate and fluid when there are no cavitations along the interface. Therefore

$$(\partial\varphi/\partial\bar{z})_{\bar{z}=0}=-W(r,\theta) \tag{17}$$

For the fluid in contact with the rigid lateral wall of the container, the fluid velocity in the radial direction is zero, so

$$(\partial\varphi/\partial r)_{r=a}=0 \tag{18}$$

The fluid free surface condition is described by the zero dynamic pressure condition at $\bar{z}=H$ as

$$(\varphi)_{\bar{z}=H}=0 \tag{19}$$

It is also useful to introduce the Rayleigh quotient (Zhu 1994) as

$$\omega^2=\frac{U_P+U_E+U_I}{T_P^*+T_L^*} \tag{20}$$

where ρ_L is the fluid mass density, χ is the direction outward normal to the boundary surface S of the fluid domain, $S=S_1+S_2$, S_1 is the shell lateral surface, S_2 is the plate surface. Using boundary conditions, the simplified reference kinetic energy T^*_L of the fluid is (Amabili 1997).

$$T_L^*=\frac{1}{2}\rho_L\iint_{S_1+S_2}\varphi\frac{\partial\varphi}{\partial\chi}dS=\frac{1}{2}\rho_L\iint_{S_1}\varphi\frac{\partial\varphi}{\partial r}dS-\frac{1}{2}\rho_L\iint_{S_2}\varphi\frac{\partial\varphi}{\partial\bar{z}}dS=\frac{1}{2}\rho_L\iint_{S_2}\varphi W dS \tag{21}$$

The fluid deformation potential φ is assumed to be of the form

$$\varphi = \sum_{i=0}^{\infty} q_i \Phi_i \tag{22}$$

The functions Φ_i for axisymmetric modes (n=0), are expressed as (Amabili 1997)

$$\Phi_i(r,\theta,\bar{z}) = \mathrm{X}_{0i0}(\bar{z}-H) + \sum_{k=1}^{\infty} \mathrm{X}_{0ik} J_0(\varepsilon_{0k} r/a)\left[\cosh(\varepsilon_{0k}\bar{z}/a) - \frac{\sinh(\varepsilon_{0k}\bar{z}/a)}{\tanh(\varepsilon_{0k}H/a)}\right] \tag{23}$$

and, for axisymmetric (n>0) modes, as

$$\Phi_i(r,\theta,\bar{z}) = \cos(n\theta)\sum_{k=1}^{\infty} \mathrm{X}_{nik} J_n(\varepsilon_{nk} r/a)\left[\cosh(\varepsilon_{nk}\bar{z}/a) - \frac{\sinh(\varepsilon_{nk}\bar{z}/a)}{\tanh(\varepsilon_{nk}H/a)}\right] \tag{24}$$

where ε_{nk} are solutions of the equation

$$J_n'(\varepsilon_{nk}) = 0, \qquad k = 1,\ldots \quad ,\infty \tag{25}$$

upon rejecting the first solution ε=0 for n=0. Functions Φ_i satisfy Eqs. (15)-(18) and (19). The constants X_{nik} are calculated in order to satisfy boundary conditions defined in Eq. (15). For asymmetric modes

$$\sum_{k=1}^{\infty} \mathrm{X}_{nik} J_n(\varepsilon_{nk} r/a) \frac{\varepsilon_{nk}}{a\tanh(\varepsilon_{nk}H/a)} = \left[J_n\left(\lambda_{ni}\frac{r}{a}\right) + A_{ni} I_n\left(\lambda_{ni}\frac{r}{a}\right)\right] \tag{26}$$

Eq. (26) must be satisfied for $0 \le r \le a$. Multiplying Eq. (26) by $(1/a^2)J_n(\varepsilon_{nk}r/a)r$, integrating from 0 to a and using the orthogonality of the Bessel functions, we obtain

$$\mathrm{X}_{nik} = \frac{(\zeta_{nik} + A_{ni}\xi_{nik})}{\varsigma_{nk}\varepsilon_{nk}} a\tanh\left(\varepsilon_{nk}\frac{H}{a}\right) \tag{27}$$

By using Eq. (25)

$$\varsigma_{nk} = \frac{1}{a^2}\int_0^a J_n^2\left(\varepsilon_{nk}\frac{r}{a}\right) r dr \tag{28}$$

$$\zeta_{nik} = \frac{1}{a^2}\int_0^a J_n\left(\varepsilon_{nk}\frac{r}{a}\right) J_n\left(\lambda_{ni}\frac{r}{a}\right) r dr \tag{29}$$

$$\xi_{nik} = \frac{1}{a^2}\int_0^a J_n\left(\varepsilon_{nk}\frac{r}{a}\right) I_n\left(\lambda_{ni}\frac{r}{a}\right) r dr \tag{30}$$

T_L^* of the reference kinetic energy of the fluid is

$$T_L^* = \frac{1}{2}\rho_L a^3 \psi_n \sum_{i=0}^{\infty}\sum_{h=0}^{\infty} q_i q_h \sum_{k=1}^{\infty} \frac{(\zeta_{nik} + A_{ni}\xi_{nik})}{\varsigma_{nk}\varepsilon_{nk}} (\zeta_{nhk} + A_{nh}\xi_{nhk}) \tanh\left(\varepsilon_{nk}\frac{H}{a}\right) \tag{31}$$

For axisymmetric modes, Eq. (26) is replaced by

$$-\mathrm{X}_{0i0}+\sum_{k=1}^{\infty}\mathrm{X}_{0ik}J_0\left(\varepsilon_{0k}\frac{r}{a}\right)\frac{\varepsilon_{0k}}{a\tanh\left(\varepsilon_{0k}H/a\right)}=\left[J_0\left(\lambda_{0i}\frac{r}{a}\right)+A_{0i}I_0\left(\lambda_{0i}\frac{r}{a}\right)\right] \tag{32}$$

The constant X_{0i0} is given by

$$\mathrm{X}_{0i0}=-\frac{2}{a^2}\int_0^a\left[J_0\left(\lambda_{0i}\frac{r}{a}\right)+A_{0i}I_0\left(\lambda_{0i}\frac{r}{a}\right)\right]rdr=-\frac{1}{2\lambda_{0i}}\left[J_1\left(\lambda_{0i}\right)+A_{0i}I_1\left(\lambda_{0i}\right)\right] \tag{33}$$

The constants X_{0ik}, for $k>0$ and $n=0$, are obtained from Eq. (27). For axisymmetric modes, the term T_L^* of the reference kinetic energy of the fluid is given by

$$T_L^*=\frac{1}{2}\rho_L a^3\psi_n\sum_{i=0}^{\infty}\sum_{h=0}^{\infty}q_iq_h\left[\frac{1}{2}\frac{H}{a}\mathrm{X}_{0i0}\mathrm{X}_{0h0}+\sum_{k=1}^{\infty}\frac{\left(\zeta_{0ik}+A_{0i}\xi_{0ik}\right)}{\varsigma_{0k}\varepsilon_{0k}}\left(\zeta_{0hk}+A_{0h}\xi_{0hk}\right)\tanh\left(\varepsilon_{0k}\frac{H}{a}\right)\right] \tag{34}$$

2.4 The eigenvalue problem

For numerical calculation of the natural frequencies and Ritz expansion parameters, only N terms in the expansion of W, Eq. (3), are considered, where N is chosen large enough to give the required accuracy. All the energy terms are given by finite summations. By introducing a vectorial notation, the vector $\mathbf{q}$ of the parameters of the Ritz expansions are defined by

$$\mathbf{q}=\begin{Bmatrix}q_0\\ \vdots\\ q_N\end{Bmatrix} \tag{35}$$

The maximum potential energy of the plate, Eq. (9) can be written as (Askari and Daneshmand 2010)

$$U_P=\frac{1}{2}\psi_n\mathbf{q}^T\mathbf{K}^P\mathbf{q} \tag{36}$$

where the elements of the diagonal matrix $\mathbf{K}^P$ are given by

$$\mathbf{K}_{ih}^P=\delta_{ih}\frac{1}{a^2}\left(\frac{E_ch^3}{12(1-\nu^2)}+\frac{h^3(E_m-E_c)(p^2-p+2)}{4(1-\nu^2)(p+1)(p+2)(p+3)}\right)\lambda_{ni}^4 \qquad i,h=1,\ldots\quad,N \tag{37}$$

The maximum potential energy stored by the Winkler elastic foundation, Eq. (11), is written as

$$U_E=\frac{1}{2}\psi_n\mathbf{q}^T\mathbf{K}^E\mathbf{q} \tag{38}$$

where $\mathbf{K}^E=k'a^2[\mathbf{I}]$, and $[\mathbf{I}]$ is the identity matrix of $N\times N$.

The maximum potential energy stored by the plate as a consequence of the in-plane load, Eq. (21), is

$$U_I = \frac{1}{2}\psi_n \mathbf{q}^T \mathbf{K}^I \mathbf{q}, \tag{39}$$

where, (for i, j=0,…,N)

$$\mathbf{K}^I_{ih} = \frac{\lambda_{ni}\lambda_{nh}}{a^2}\int_0^a N_{ipl}\left[A_{ni}J'_n\left(\lambda_{ni}\frac{r}{a}\right)+C_{ni}I'_n\left(\lambda_{ni}\frac{r}{a}\right)\right]\times\left[A_{nh}J'_n\left(\lambda_{nh}\frac{r}{a}\right)+C_{nh}I'_n\left(\lambda_{nh}\frac{r}{a}\right)\right]rdr + n^2\int_0^a N_{ipl}\left[A_{ni}J_n\left(\lambda_{ni}\frac{r}{a}\right)+C_{ni}I_n\left(\lambda_{ni}\frac{r}{a}\right)\right]\times\left[A_{nh}J_n\left(\lambda_{nh}\frac{r}{a}\right)+C_{nh}I_n\left(\lambda_{nh}\frac{r}{a}\right)\right]\frac{dr}{r} \tag{40}$$

The reference kinetic energy of the plate, Eq. (7), is written as

$$T_P^* = \frac{1}{2}\psi_n \mathbf{q}^T \mathbf{M}^P \mathbf{q} \tag{41}$$

where

$$\mathbf{M}^P = \left(\rho_c h + \frac{h(\rho_m - \rho_c)}{(p+1)}\right)a^2[\mathbf{I}] \tag{42}$$

[**I**] is the $N\times N$ identity matrix. The simplified reference kinetic energy of the fluid, given in Eq. (21), can be written as

$$T_L^* = \frac{1}{2}\psi_n \mathbf{q}^T \mathbf{M}^L \mathbf{q} \tag{43}$$

The elements of the matrix $\mathbf{M}^L$ of dimension $N\times N$ are given by

$$\mathbf{M}^L_{ih} = \rho_L a^3 \sum_{k=1}^{\infty}\frac{(\zeta_{nik} + A_{ni}\xi_{nik})}{\varsigma_{nk}\varepsilon_{nk}}(\zeta_{nhk} + A_{nh}\xi_{nhk})\tanh\left(\varepsilon_{nk}\frac{H}{a}\right) \qquad for \quad i,h = 0,... \quad ,N \tag{44}$$

For axisymmetric modes (n=0) the matrix $\mathbf{M}^L$ should be changed to

$$\mathbf{M}^L_{ih} = \rho_L a^3\left[\frac{1}{2}\frac{H}{a}\mathrm{X}_{0i0}\mathrm{X}_{0h0} + \sum_{k=1}^{\infty}\frac{(\zeta_{0ik} + A_{0i}\xi_{0ik})}{\varsigma_{0k}\varepsilon_{0k}}(\zeta_{0hk} + A_{0h}\xi_{0hk})\tanh\left(\varepsilon_{0k}\frac{H}{a}\right)\right] \quad for \quad i,h = 0,...,N \tag{45}$$

By substituting Eqs. (37)-(38)-(39)-(41) and (43) into the Rayleigh quotient, Eq. (20), and minimizing with respect to the coefficient q_i, we can finally obtain

$$(\mathbf{K}^P + \mathbf{K}^E + \mathbf{K}^I)\mathbf{q} - \Omega^2(\mathbf{M}^P + \mathbf{M}^L)\mathbf{q} = 0 \tag{46}$$

in which Ω is the circular frequency of the fluid-coupled system. Eq. (46) gives a linear eigenvalue problem for a real, non-symmetric matrix.

3. Numerical results

Using the preceding analysis, the eigenvalue problem, Eq. (46) is solved to find the natural

Table 1 Material properties used for the FGM plate

Properties	Metal	Ceramic	
	Aluminum (Al)	Zirconia (ZrO_2)	Aluminia (Al_2O_3)
E (GPa)	70	200	380
ρ (Kg/m^3)	2702	5700	3800

Table 2 Effects of M on convergence of natural frequencies (Hz). (N=5, H=a, k'=10^5, Al/ZrO_2, p=2)

Mode		M			
n	m	2	3	4	5
0	0	82.31	82.22	82.21	82.21
	1	558.63	479.84	478.44	478.27
1	0	225.16	224.98	224.96	224.96
	1	959.62	828.66	826.78	826.56
2	0	433.05	432.48	432.43	432.43
	1	1469.42	1256.46	1253.15	1252.75
3	0	699.97	698.77	698.66	698.64
	1	2058.35	1753.63	1748.64	1747.96
4	0	1025.15	1023.09	1022.87	1022.83
	1	2720.45	2317.99	2311.09	2310.05

Table 3 Effect of N on convergence of natural frequencies (Hz). (M=5, H=a, k' = 10^5, Al/ZrO_2, p=2)

Mode		M			
n	m	2	3	4	5
0	0	82.28	82.22	82.21	82.21
	1	581.02	478.76	478.38	478.27
1	0	225.11	224.99	224.97	224.96
	1	831.22	827.54	826.79	826.56
2	0	432.67	432.49	432.44	432.43
	1	1257.70	1253.88	1253.02	1252.75
3	0	698.97	698.74	698.67	698.64
	1	1752.91	1749.17	1748.24	1747.96
4	0	1023.23	1022.95	1022.86	1022.83
	1	2314.89	2311.29	2310.34	2310.05

frequencies and mode shapes of a FGM flexible circular plate resting on a Winkler elastic foundation. Experimental and numerical results available in the literature and a commercial finite element code (ABAQUS) are used to validate the results of the present study. Quadrilateral shell elements (S4R) are used for the finite element model of the structure. This element is a four-node, doubly curved shell element with reduced integration, hour-glass control, and finite membrane strain formulation. Acoustic three-dimensional elements (AC3D8) based on linear wave theory are also used for the fluid. The elements are solid, eight-node brick acoustic elements with linear interpolation and with only one pressure unknown per node. The location of each node on the constrained surfaces of the fluid corresponds exactly to the location of a node on the structure.

Table 4 Coupled natural frequencies (Hz) for $H=a$, $k' = 10^5$ and $p=2$

Mode	Al/ZrO_2		Al/Al_2O_3	
	This study	FEM	This study	FEM
1st	82.21 (0,0)*	79.65	107.56 (0,0)	103.57
2nd	224.96 (1,0)	216.65	298.93 (1,0)	286.33
3rd	432.43 (2,0)	415.33	582.42 (2,0)	564.48
4th	478.27 (0,1)	466.91	643.65 (0,1)	615.16
5th	698.64 (3,0)	667.65	950.27 (3,0)	919.88
6th	826.56 (1,1)	807.64	1124.40 (1,1)	1086.61

*(n,m)

Surface tied normal contact was considered between the surfaces of the fluid and tank walls. No sloshing waves are considered in this study. In the present finite element model, the circular plate is divided into 3200 shell elements of the different size whereas the fluid region consists of 12880 fluid elements. In numerical analysis, the plate is assumed to be made of functionally graded material with properties given in Table 1. v=0.3 and also for validations are used steel with Young's modulus E=206 Gpa, Poisson's ratio v=0.25 and mass density ρ_L=7850 Kg/m^3. The fluid is water with mass density ρ_L=1000 Kg/m^3. The plate has a radius a=0.114 m and a wall thickness h=0.002 m. The cylindrical tank is filled to H with L=0.2 m.

3.1 Convergence and validity study

In order to check the convergence of the developed method, an elastic clamped FGM plate of a partially water-filled rigid tank is analyzed. Tables 2-3 show the convergence of the theoretical method for different number of terms used in the series expansions. It is observed that five terms for plate modes (N=5) in the Ritz expansion, Eqs. (3)-(5), and five terms (M=5) in the expansions of Φ_i, Eqs. (23)-(24), have been enough for good accuracy.

To validate the semi-analytical method developed in the present study, the results are compared with those obtained from the finite element analysis in Table 4. As seen, the agreement between the results is good and the largest discrepancy is less than 4.4 %. Tables 5-6 compare the results of this study with those of obtained by Askari and Daneshmand (2010), Chiba (1992) and Ergin and Uğurlu (2004) whereas they considered the steel plate. It should be noted that the results for both including and neglecting the effect of in-plane force are provided in Tables 5-6. A good agreement between the results can be seen. However, there are some differences between the results of the present study and those found in the literature. In addition to those discrepancies discussed, if neglected the effect of in-plane force in calculation, the largest discrepancy will be less than 0.11% for all filling ratios with the predictions of Askari and Daneshmand (2010). This difference when the effect of in-plane force taken into account increases by 0.17% for $H=0.1\ L$ and reaches to 3.91% for $H=2\ L$. it might be because the effect of in-plane force is neglected by Askari and Daneshmand (2010). As seen from these tables, discrepancies raise with increasing the fluid-filling ratio. This comes from the decrease of the effect of in-plane forces in the bottom plate with the increase of filling ratio. The largest discrepancy is less than 2.45% and 1.28% compared with experimental data reported by Chiba (1992) and numerical one presented by Ergin and Uğurlu (2004), respectively.

Table 5 Coupled natural frequencies (Hz) for the coupled system

Mode		H/a=0.1					H/a=0.5				
m	n	This study[1]	This study[2]	Askari and Daneshmand (2010)	Chiba (1992)	Ergin and Uğurlu (2004)	This study[1]	This study[2]	Askari and Daneshmand (2010)	Chiba (1992)	Ergin and Uğurlu (2004)
0	0	174.2	173.9	173.9	177	173.5	112.7	112.7	112.7	110	112.8
0	1	364.6	364.4	364.4		365.7	262.9	262.2	262.2		264.6
1	0	689.2	689.1	689.1	694	688.1	539.6	538.7	538.6	540	540.6
1	1	1067.2	1066.2	1066.1		1072.3	893.2	892.2	891.9		902.5
2	0	1584.5	1583.4	1583.0	1620	1585.2	1390.4	1387.3	1386.2	1410	1393.9
2	1	2164.2	2162.4	2162.2		2183.0	1976.3	1963.0	1962.2		1991.3

[1]Including the effect of in-plane force due to the weight of the fluid
[2]Neglecting the effect of in-plane force due to the weight of the fluid

Table 6 Coupled natural frequencies (Hz) for the coupled system

Mode		H/a=1					H/a=2			
m	n	This study[1]	This study[2]	Askari and Daneshmand (2010)	Chiba (1992)	Ergin and Uğurlu (2004)	This study[1]	This study[2]	Askari and Daneshmand (2010)	Ergin and Uğurlu (2004)
0	0	91.7	90.3	90.30	92	91.3	71.8	69.1	69.1	71.8
0	1	246.7	244.3	244.30		247.4	245.9	241.0	241.0	244.2
1	0	515.3	511.7	511.60	520	515.1	505.9	495.8	495.7	499.5
1	1	879.8	875.3	874.90		886.3	887.4	872.1	872.1	883.6
2	0	1369.9	1364.4	1363.00	1390	1372.3	1369.2	1351.7	1350.2	1356.2
2	1	1961.9	1949.5	1947.40		1976.9	1963.0	1944.5	1945.0	1974.5

[1]Including the effect of in-plane force due to the weight of the fluid
[2]Neglecting the effect of in-plane force due to the weight of the fluid

3.2 The number of nodal diameter n

The variations of normalized natural frequencies for the coupled system as a function of the number of nodal diameters n are shown in Fig. 3. The normalized natural frequency is defined as the coupled natural frequency divided by the natural frequency of the plate in vacuum for the specific corresponding mode. Fig. 3 shows that the frequencies increase as the number of nodal diameters n enhances. It might be worthy to note that for a given number of nodal diameter n, the frequencies increase as the number of nodal circles m increase. Therefore the fundamental frequency always belongs to the curve m=0. For each number of nodal circles m, the minimum values of normalized natural frequencies occur for n=0.

3.3 Functionally graded material

The effect of a wide range of material parameter on the natural frequencies for m=0 and m=1 and different nodal diameters (n) are investigated in Figs. 4-5, respectively. It can be seen from

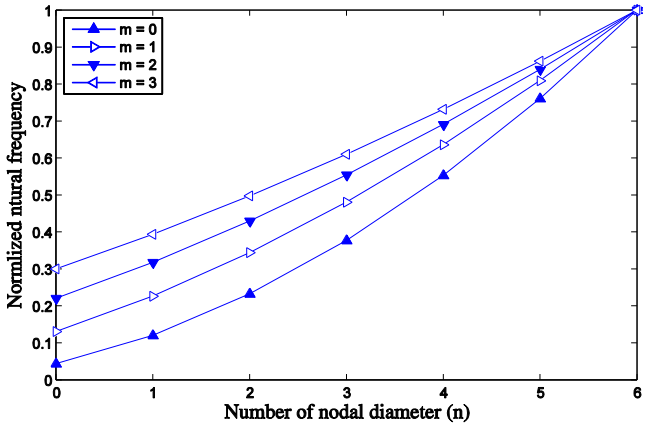

Fig. 3 Normalized natural frequencies with respect to the number of nodal diameter n for the coupled system for $H=a$, $k' = 10^5$ and Al/ZrO_2 material with $p=2$

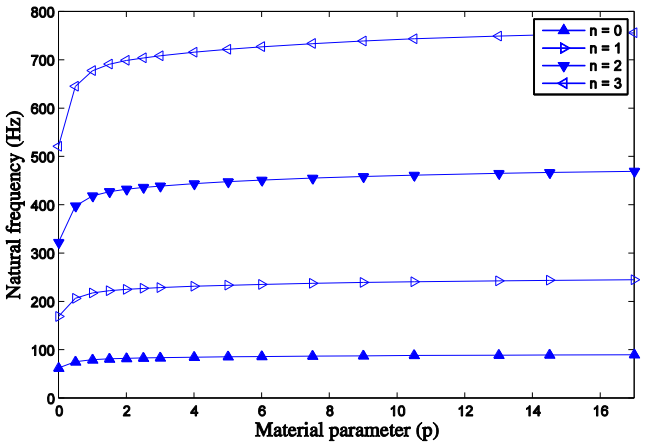

Fig. 4 Natural frequencies of the coupled system as a function of material parameter (p) for $H=a$, $k' = 10^5$ and $m=0$

these figures that the natural frequencies increase as the material parameter increase. It is because raising the material parameter changes the dominant material properties of the plate from ceramic to Al. In order to clarify this fact it should be noted that when p is 0, the plate behaves as a metal (Al), however, as the value of p goes to infinity, the plate behavior goes towards ZrO_2. The main increase in natural frequencies can be seen between $p=0$ and 5. It should be noted that the raising of the material parameter has more effects on natural frequencies obtained for $m=1$ than those for $m=0$.

3.4 Winkler elastic foundation

The presence of a Winkler elastic foundation is now considered for the same tank completely filled by water and with the material parameter $p=2$ in Fig. 6 The stiffness of Winkler foundation

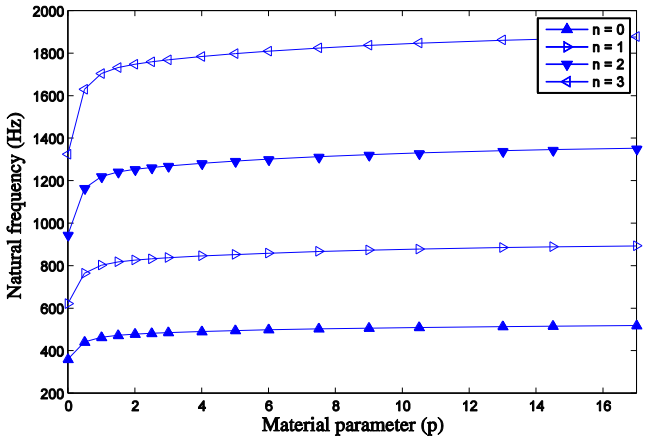

Fig. 5 Natural frequencies of the coupled system as a function of material parameter (p) for $H=a$, $k' = 10^5$ and $m=1$

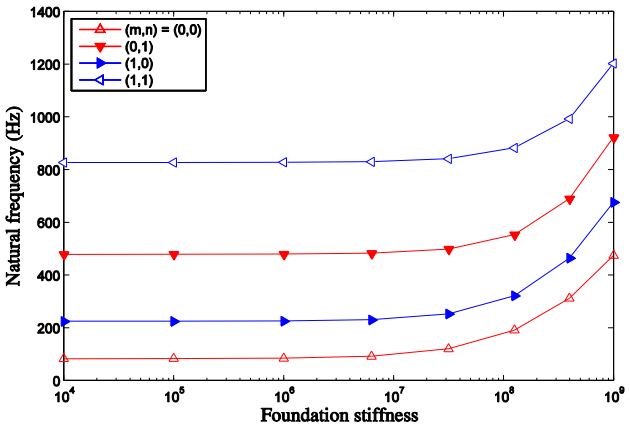

Fig. 6 Effect of the foundation stiffness k' on the natural frequencies of the coupled system for $H=a$ and Al/ZrO_2 material with $p=2$

has no effects on the natural frequencies of the plate since the stiffness of foundation is too small compared with the plate stiffness when it is lower than 10^6 N/m^3. After that, increasing the foundation stiffness raises the natural frequencies of the fluid-coupled system exponentially. The upward trends of natural frequencies are similar for curves with different circumferential mode numbers as it can be seen in figure.

3.5 The fluid level

The variation of the first three natural frequencies as a function of filling ratio (H/L) for the Al/$AlZrO_2$-plate with different thicknesses, h=0.7, 1, and 2 mm are shown in Figs. 7, 8 and 9, respectively. Two types of conditions were considered for including (Type I) and neglecting (Type II) the effect of in-plane force due to the weight of the fluid. The results are represented by dash-

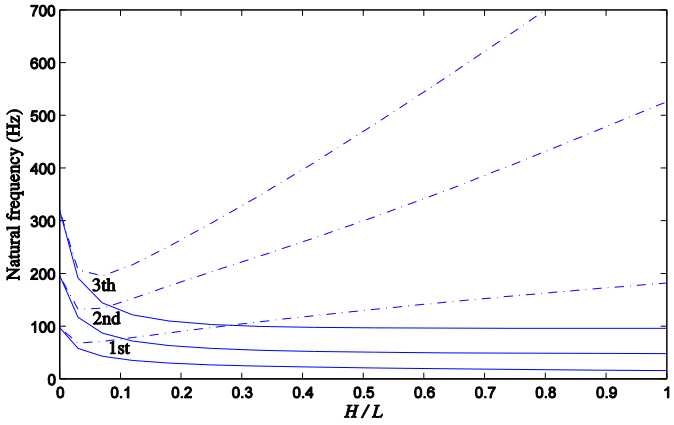

Fig. 7 Variation of the first three modes with *H/L*, *h*=0.7 mm, – · – · – Type I condition, —— Type II condition, $k' = 10^5$, Al/ZrO_2, *p*=2

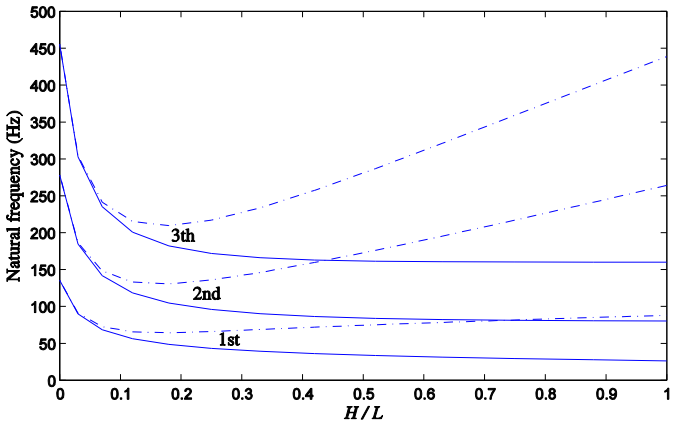

Fig. 8 Variation of the first three modes with *H/L*, *h*=1 mm, – · – · – Type I condition, —— Type II condition, $k' = 10^5$, Al/ZrO_2, *p*=2

dotted lines and solid lines for type I and type II, respectively.

In type I condition with plate thickness *h*=0.07 mm, the natural frequencies decrease sharply in the range of $0<H/L<0.05$ due to the increase of the added mass effect of the fluid on the bottom plate motion. Further increase of *H/L* causes the natural frequencies to increase on account of the increase of the effect of in-plane forces of the bottom plate. The in-plane force effect is dominant with respect to added mass effect for $H/L>0.05$. In type II conditions for *h*=0.07 mm, the natural frequencies decrease sharply in the range of $0<H/L<0.1$. Further increase of *H/L* leads to the natural frequencies continuing to decrease because the effect of in-plane force is neglected in this case. The effect of fluid level is very small in filling ratios $H/L>0.4$. In each mode, type II natural frequencies are lower than those of type I, however, the difference between natural frequencies in Type I and II, increase with increasing filling ratio and mode number. Next, for the larger value of the thickness of the plate, i.e., *h*=1 mm shown in Fig. 8, the increase in the natural frequencies with

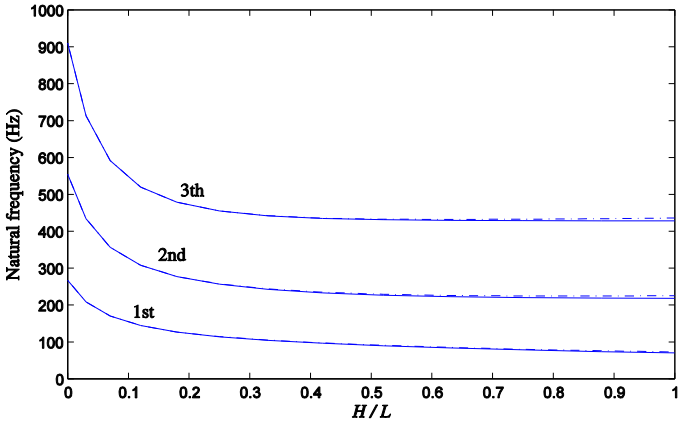

Fig. 9 Variation of the first three modes with H/L, h=2 mm, – · – · – Type I condition, —— Type II condition, $k' = 10^5$, Al/ZrO_2, p=2

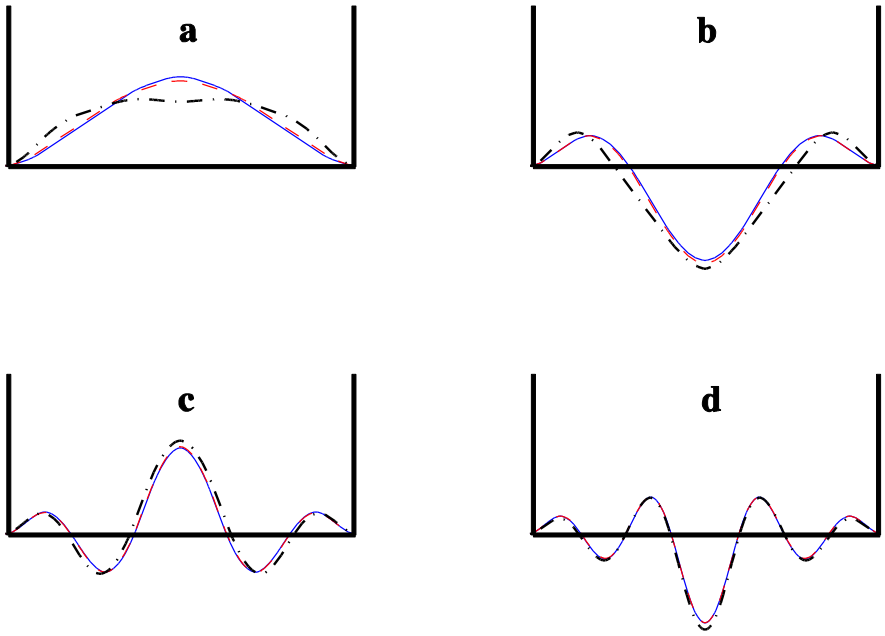

Fig. 10 First four modes (n = 0 and H=a, p=2) for different values of foundation stiffness. (a)m = 0; (b) m = 1; (c) m = 2; (d) m = 3 (—— k'=10^5, – – – k'=10^8, – · – · – k'=10^{10})

H/L for Type I is less than those obtained for h=0.07. It seems to occur due to the decrease in the effect of in-plane forces of the plate with increasing the thickness. In the case of h=2 mm shown in Fig. 9, there is a little difference in the values among two types of conditions (I and II) whereas no increase in the natural frequencies can be seen for type I.

Generally, when the plate is thin especially in high filling ratio, which results in large static deflections, one must consider in-plane forces but for higher thickness, it is not very significant as much as ignorable in the calculations.

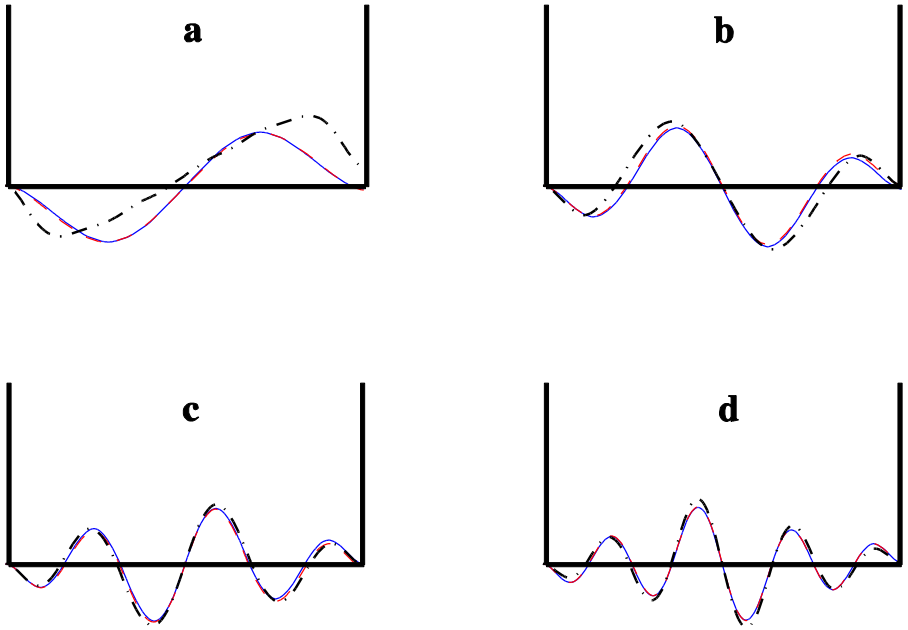

Fig. 11 First four modes (n = 1 and H=a, p=2) for different values of foundation stiffness (a) m = 0; (b) m = 1; (c) m = 2; (d) m = 3 (—— k'=10^5, – – – k'=10^8, – · – · – k'=10^{10})

3.6 Vibration mode shapes

The first four mode shapes of the FGM elastic plate coupled with the fluid for different values of (k') having the number of nodal diameters n=0 and 1 are shown in Figs. 10-11, respectively. The mode shapes are plotted in the tank section defined by θ=0 and θ=π. As it can be observed from these figures, the locations of the nodal points (the points with zero displacement) and peak points change with k' which means the mode shapes vary with foundation stiffness. The effect of foundation stiffness on the axisymmetric mode shapes (n=0) is more than its effect on the asymmetric mode shapes (n>0). Near the centerline, foundation stiffness has more effect on the mode shapes and the effect of foundation stiffness on the mode shapes decrease as the number of nodal circles m increase.

4. Conclusions

Hydroelastic vibration of functionally graded circular plates resting on Winkler elastic foundations, including the effects of both in-plane forces due to fluid weight and the interaction between fluid and plate, was theoretically investigated. Results obtained by the proposed approach were validated by the experimental and numerical data available in the literature. Effects of fluid level, functionally graded material, elastic foundation stiffness, and numbers of nodal diameter and circle (n, m) on the natural frequencies and the mode shapes of the coupled system were also considered.

It was found that by increasing the material parameter, the natural frequencies of the fluid-

coupled system increase; however, this increase for the greater amount of material parameter is lower than those with smaller ones. Also, it was observed that the natural frequency of the plate increases as the elastic foundation stiffness increases.

Effects of fluid level on the natural frequencies of the FGM elastic plate resting on an elastic foundation vary with number of nodal diameters and circles (*n,m*), i.e., these effects are stronger for modes with smaller number of nodal diameters and circles. The natural frequencies by taking in-plane forces into account are higher than those that neglect this effect, however, the difference between natural frequencies, increase with increasing filling ratio and mode number.

References

Aliaga, J.W. and Reddy, J.N. (2004), "Nonlinear thermoelastic analysis of functionally graded plates using the third-order shear deformation theory", *Int. J. Comput. Eng. Sci*., **5**, 753-779.

Allahverdizadeh, A., Naei, M.H. and Nikkhah Bahrami, M. (2008), "Nonlinear free and forced vibration analysis of thin circular functionally graded plates", *J. Sound. Vib.*, **310**(4-5), 966-984.

Amabili, M. (1997), "Shell-plate interaction in the free surface vibration of circular cylindrical tanks partially filled with a liquid: the artificial spring method", *J. Sound. Vib.*, **199**(3), 431-452.

Amabili, M. and Dalpiaz, G. (1998), "Vibrations of base plates in annular cylindrical tanks: theory and experiments", *J. Sound. Vib.*, **210**(3), 329-350.

Askari, E. and Daneshmand, F. (2010), "Free vibration of an elastic bottom plate of a partially fluid-filled cylindrical container with an internal body", *Eur. J. Mech. A-Solid*., **29**(1), 68-80.

Bouderba., B., Houari., M.S.A. and Tounsi., A. (2013), "Thermomechanical bending response of FGM thick plates resting on Winkler-Pasternak elastic foundations", *Steel Compos. Struct*., **14**(1), 85-104.

Chan Il, P. (1992), "Hydroelastic vibration of a cylindrical tank with an elastic bottom, containing liquid. Part I: experiment", *J. Fluid. Struct.*, **313**(1-2), 325-333.

Chen, W.R., Chen, C.S. and Yu, S.Y. (2011), "Nonlinear vibration of hybrid composite plates on elastic foundations", *Struct. Eng. Mech*., **37**(4), 367-383.

Chiba, M. (1992), "Nonlinear hydroelastic vibration of a cylindrical tank with an elastic bottom, containing liquid. Part I: Experiment", *J. Fluid. Struct.*, **6**(2), 181-206.

Chun-Sheng, C. (2005), "Nonlinear vibration of a shear deformable functionally graded plate", *Compos. Struct*., **68**(3), 295-302.

Ebrahimi, F., Sepiani, H. and Ghorbanpour Arani , A. (2011), *Progress in Analysis of Functionally Graded Structures*, Nova Science, United States.

Ergin, A. and Uğurlu, B. (2003), "Linear vibration analysis of cantilever plates partially submerged in fluid", *J. Fluid. Struct*., **17**(7), 927-939.

Ergin, A. and Uğurlu, B. (2004), "Hydroelastic analysis of fluid storage tanks by using a boundary integral equation method", *J. Sound. Vib.*, **275**(3-5), 489-513.

Gunaratnam, D.J. and Bhattacharya, A.P. (1985), "Transverse vibration of circular plates having mixed elastic rotational edge restraints and subjected to in-plane forces", *J. Sound. Vib.*, **102**(3), 431-439.

Hosseini-Hashemi, S., Rokni Damavandi Taher, H., Akhavan, H. and Omidi, M. (2010), "Free vibration of functionally graded rectangular plates using first-order shear deformation plate theory", *Appl. Math. Model.*, **34**(5), 1276-1291.

Jain, R.K. (1972), "Vibrations of circular plates of variable thickness under an inplane force", *J. Sound. Vib.*, **23**(4), 407-414.

Jeong, K.H. (2003), "Free vibration of two identical circular plates coupled with bounded fluid", *J. Sound. Vib.*, **260**(4), 653-670.

Kutlu, A., Uğurlu, B., Omurtag, M.H. and Ergin, A. (2012), "Dynamic response of Mindlin plates resting on arbitrarily orthotropic Pasternak foundation and partially in contact with fluid", *Ocean Eng*., **42**, 112-125.

Leissa, A.W. (1969), Vibration of Plates, NASA SP 160U.S. Government Printing Office, Washington, DC.
Nie, G.J. and Zhong, Z. (2007), "Semi-analytical solution for three-dimensional vibration of functionally graded circular plates", *Comput. Method. Appl. M.*, **196**(49-52), 4901-4910.
Rad, A.B. (2012), "Static response of 2-D functionally graded circular plate with gradient thickness and elastic foundations to compound loads", *Struct. Eng. Mech*., **44**(2), 139-161.
Shen, H.S. (2009), *Functionally Graded Materials: Nonlinear Analysis of Plates and Shells*, CRC Press, Boca Raton.
Yang, J. and Shen, H.S. (2001), "Dynamic response of initially stressed functionally graded rectangular thin plates", *Compos. Struct*., **54**(4), 497-508.
Zhu, F. (1994), "Rayleigh quotients for coupled free vibrations", *J. Sound. Vib*., **171**(5), 641-649.